SIMPLIFIED TECHNIQUES FOR PREDICTING VIBRO-ACOUSTIC ENVIRONMENTS

K. Y. Chang and G. C. Kao
Wyle Laboratories
Huntsville, Alabama 35807

ABSTRACT

A simplified method has been developed to predict broad frequency range vibration criteria which account for both primary and component load impedance for structures excited by random acoustic excitations. The vibro-acoustic environments were predicted by a one-dimensional equation which utilizes four types of parameters at equipment mounting locations. These parameters consist of input impedance of support structure, acoustic mobility of structural system, input impedance of component package, and blocked pressure spectrum. A set of nomograms and design charts was developed to evaluate the force response graphically with minimum amount of manual computation. The accuracy of the equation in predicting force responses has been verified satisfactorily and the method has proved to be a practical and useful preliminary design tool for aerospace vehicles. Two example problems with different structural configurations were used to demonstrate computation procedures. Satisfactory agreements between analytical predictions and experimental measurements were observed.

INTRODUCTION

The prediction of localized vibratory criteria for space vehicle components due to acoustic excitation has been accomplished based on the empirical techniques as described in Reference 1. These techniques provide standardized approaches to predict vibro-acoustic environments with sufficient conservatism to satisfy design and test requirements for unloaded primary structures. The testing of components to such criteria is valid only when the impedance of a primary structure is sufficiently higher than that of the attached component. Otherwise, there is a strong possibility that the specimen would be overtested.

A complementary technique by which the vibratory criteria are to be specified in terms of actual forces acting on components has been considered [2]. Test specifications are given in terms of the power spectral density of a force environment which account for the effects of component-primary structure coupling and the approach is designated as the "Force-Spectrum" method. This approach requires sophisticated measurement techniques to define the dynamic parameters required for the prediction equation. The objective of this paper is to present a simplified computation procedure to allow performance of quick estimates on force spectra. It is recognized that several analytical methods, such as the direct integration method and other numerical methods, can be used for the prediction of loads on finite cylindrical structures. Nevertheless, the resulting equations are either too sophisticated or too general and are not practical for performing quick estimates with adequate accuracies. Considering the fact that an average engineer does not have ample time to thoroughly analyze each individual problem; therefore, simplified methods are needed to solve complex problems with a minimum amount of calculations and yet provide adequate accuracy. This is accomplished by the use of charts and nomograms to reduce complex computations.

FORCE-SPECTRA EQUATIONS

The force-spectra equation is derived based on a one-dimensional structural impedance model [2]. By applying Thevenins' and Norton's theorems to this model, the equation which relates the force-spectra to external excitation forces, component impedance and dynamic properties of support structures, such as structural impedances and acoustic mobilities, is established. The final equation is obtained as follows:

$$\Phi_L(\omega) = \left| \frac{Z_L Z_S}{Z_L + Z_S} \right|^2 \cdot \left| \alpha(\omega) \right|^2 \cdot \Phi_P(\omega) \qquad (1)$$

where $\Phi_L(\omega)$ = Predicted driving force spectrum

$Z_S(\omega)$ = Input impedance of primary structures

$Z_L(\omega)$ = Input impedance of component

$\alpha(\omega)$ = Acoustic mobility of primary structure

$\Phi_P(\omega)$ = Blocked sound pressure spectrum

Due to structural complexities of space vehicles, precise analytical approaches to obtain the parameters defined above are not practical. Therefore, in order to validate Equation (1), approximate equations along with measured data were used to predict the force spectra quantitatively.

An alternate approach to compute the driving force spectrum could be achieved by replacing the produce of $\left| \alpha(\omega) \right|^2 \cdot \Phi_P(\omega)$ by $\Phi_R(\omega)$, which is defined as the velocity response spectrum at the component mounting points of the unloaded primary structure. Thus, Equation (1) can be written as follows:

$$\Phi_L(\omega) = \left| \frac{Z_L Z_S}{Z_L + Z_S} \right|^2 \cdot \Phi_R(\omega) \qquad (2)$$

and this spectrum may be acquired from the available experiments on the selected test specimens. A flow chart indicating the computation sequence to determine the force spectra is explained in Figure 1.

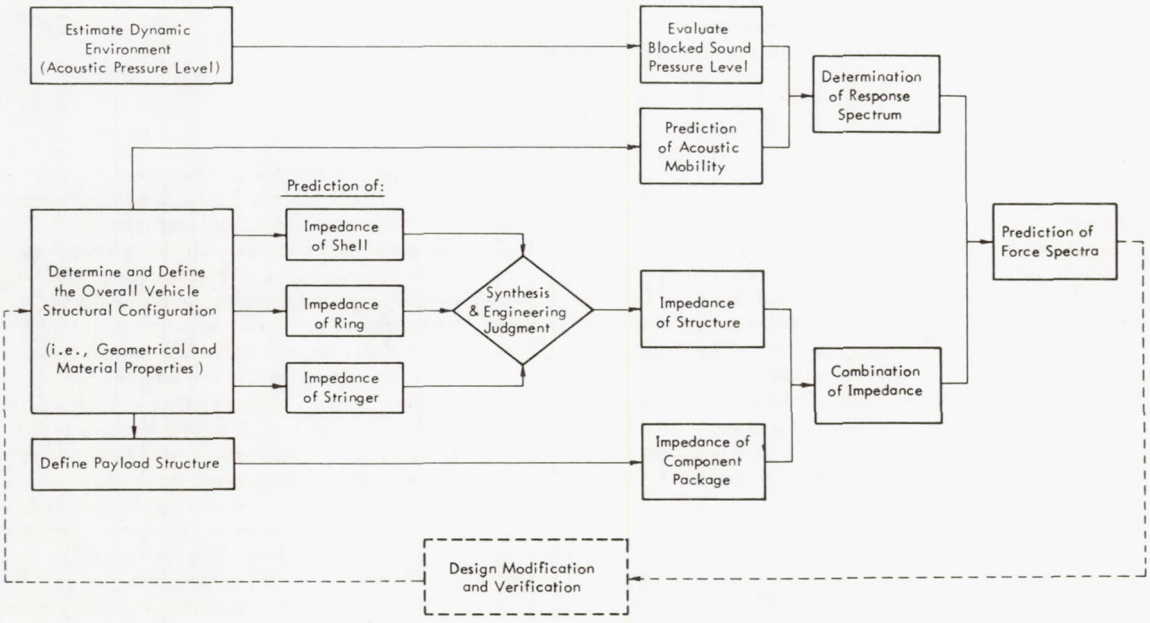

Figure 1. Flow Chart for Predicting the Force Spectra of Structures

TABLE 1. SUMMARY OF INPUT-IMPEDANCE EQUATIONS OF BEAMS, RINGS AND SHELLS

Structure / Frequency	Beam	Ring	Shell	Stiffened Shell
Low Frequency Range $\left(f \le f_L\right)$	$K_B = \frac{48\,EI}{\ell^3}$	$K_R = \frac{EI}{0.15R^3}$	$K_S = 2.5Eh\left(\frac{R}{\ell}\right)^{1/2}\left(\frac{h}{R}\right)^{1.25}$	$K = K_S + \sum K_B$ (or $+ \sum K_R$) $\lvert Z\rvert = K/\omega$
Fundamental Frequency, f_L	$\frac{1}{2\pi}\left(\frac{\pi}{\ell}\right)^2\sqrt{\frac{EI}{\rho A}}$	$\frac{0.427}{R^2}\sqrt{\frac{EI}{\rho A}}$	$\frac{0.375}{\ell}\sqrt{\frac{Eh}{\rho R}}$	
Intermediate Frequency Range $\left(f_L < f \le f_R\right)$	$Z_B = 2(1+i)\rho A \cdot \left[\frac{EI}{\rho A}\right]^{1/4}\sqrt{\omega}$	$Z_R = i2\sqrt{2}\,\rho A \cdot \left[\frac{EI}{\rho A}\right]^{1/4}\sqrt{\omega}$	$\lvert Z_S\rvert = \frac{4}{\sqrt{3}}\rho h^2\sqrt{\frac{E}{\rho R}} \cdot \left(\frac{E}{\rho}\right)^{1/4}\frac{1}{\sqrt{\omega}}$	$Z = Z_S + \sum Z_B + \sum Z_R$
Ring Frequency, f_R			$\frac{1}{2\pi R}\sqrt{\frac{E}{\rho}}$	
High Frequency Range $\left(f > f_R\right)$	Same as Intermediate	Same as Intermediate	$Z_S = \frac{4}{\sqrt{3}}h^2\sqrt{E\rho}$	$Z = Z_S$ $Z = Z_B$ $Z = Z_R$

Input impedances in the force-spectra equation are specified in terms of the "force/velocity" format. The cylindrical type structures considered herein are stiffened by stringers in the axial direction, and ring frames are attached inside the shell wall. The direction of vibratory response under consideration is referred to as that normal to the skin which is excited by impinging acoustic pressures. The approximate equations for predicting the input impedance of the above structural components are given in Table 1 in three different frequency ranges as defined below [3]:

- Low frequency range or frequencies below the fundamental frequency of the shell,
- Intermediate frequency range, and
- High frequency range or frequencies above the ring frequency of the shell.

Therefore, the evaluation of the stiffened shell impedances is obtained for these three frequency ranges as follows:

Low Frequency Impedances — The static stiffness is the predominant factor which influences the input impedance. Due to the lack of theoretical expressions for input impedances of stiffened cylindrical shells, it is assumed that at low frequencies the input impedance at any location follows the stiffness line, this stiffness being equal to the summation of the stiffness of the individual structural elements that are present in that location. Two cases are considered in this frequency range, namely:

- If the stiffness of the ring is small in comparison to the stiffness of the stringer or the unstiffened shell, the overall stiffness can be computed by adding the stiffness of the properly modeled structural elements that are present at the input location, as follows:

$$K = K_s + \sum K_B + \sum K_R \qquad (3)$$

where K_s = static stiffness of shells

K_B = static stiffness of stringers or beams

K_R = static stiffness of rings

Thus the input impedance of a stiffened cylindrical shell at low frequency follows a stiffness line whose value can be computed from the sum of stiffnesses of structural elements at that point.

- For a stiffened cylindrical shell, if rings are sufficiently stiff in comparison with the entire shell, these rings act like the boundary of structure panels. Then the characteristic impedance of the shell can be determined from the length of the spacing between two adjacent rings.

$$K = K_s + \sum K_B \qquad (4)$$

The characteristic impedance represents the impedance of a structure of such a length that reflections from the boundaries are negligible. In other words, the resonance modes of a structure with any non-dissipative boundary conditions are identical to the resonance modes of a supported structure whose length is equal to the distance between the node lines.

Intermediate Frequency Impedances — Within the intermediate frequency range, which extends from the fundamental frequency to the ring frequency, the input impedances of the test specimens can be evaluated as the combination of the characteristic impedances of the primary structural components. The equation is written as:

$$Z = Z_s + \sum Z_B + \sum Z_R \qquad (5)$$

where Z_s = characteristic impedance of shells

Z_B = characteristic impedance of stringers

Z_R = characteristic impedance of rings

High Frequency Impedances — The input impedance of a stiffened shell at high frequencies depends on the location of a measurement point and is evaluated by the following rules:

- Unstiffened (skin) Point — The input impedance approaches that of an infinite plate of the same thickness.
- Stiffened Point — The skin and the stiffener(s) decouple dynamically at high frequencies, therefore, the input impedance approaches that of the stiffener(s).
- Stiffened Intersection Point — The input impedance at the centers of short stiffeners segments are generally higher than those of longer stiffener segments; and the impedance at an intersection of the stiffeners is approximately equal to the sum of the individual impedances of the two stiffeners — the ring impedance and stringer impedance.

Acoustic mobility, $\alpha(\omega)$, is defined as the ratio of the mean-square spectral density of the velocity of the mean-square spectral density of the fluctuating pressure driving the structure. This quantity is expressed by Equation (6) as follows:

$$\alpha(\omega) = \frac{S_{\dot{u}}(\omega)}{S_p(\omega)} \qquad (6)$$

where $S_{\dot{u}}(\omega)$ has units of $(\text{in./sec})^2/\text{Hz}$, and $S_p(\omega)$ is the blocked pressure spectral density having units of $(\text{psi})^2/\text{Hz}$. The blocked pressure includes the effects of reflection and thus accounts for the pressure doubling effect when an object is immersed in a random pressure field.

Generally, the acoustic mobility for a given structure would be calculated based upon modal analysis or statistical energy analysis. However, for the purposes of presenting simplified design curves for acoustic mobility derived from acceleration data of a wide range of vibro-acoustic measurements are shown in Figure 2 for two values of damping: $Q = 20$ and $Q = 200$ [3].

Based on the empirical curves of Figure 2, the α-term is dependent on the structural damping, Q, the diameter of the cylinder, D, and the unit surface weight, m, where f is the frequency in Hz. For structural damping values other than those shown in Figure 2, the acoustic mobility term may be interpolated since an increase in Q by a factor of 10 results in an increase in the acoustic mobility term of one decade.

The blocked pressure spectrum, $\Phi_p(\omega)$, is defined as the effective acoustic pressure acting on a primary structure. The pressure is equivalent to that acting on a rigid cylinder which has the identical geometrical dimensions as the primary structure. This pressure can be determined from the far-field sound pressure measurement and is given by [4]:

$$\beta = \frac{\left[P^2_{block}\right]}{\left[P^2_{far}\right]} = 4(\pi kR)^{-2} \sum_{m=0}^{\infty} \epsilon_m \left| H'_m(kR) \right|^{-2} \qquad (7)$$

where $\left[P_{far}\right]$ = measured sound pressure levels without the presence of flexible structures

k = wave number $= 2\pi f/c$

c = speed of sound in acoustic medium; for air $c = 13{,}400$ in./sec

R = radius of cylinder

ϵ_m = Neumann factor = 1 for $m = 0$, 2 for m 0

$H'_m(kR)$ = derivative of Hankel function of order, m

The foregoing equation is derived for an infinite panel and does not account for diffraction effects of structures with finite length. However, the error due to diffraction effects is considered as insignificant and will not influence the final results. In the frequency range of interest, the RMS blocked sound pressure is approximately 40 percent higher than the measured sound pressure and such a conversion factor generally leads to conservative estimates of the force spectra.

COMPUTATION CHARTS AND GUIDELINES

In order to minimize manual efforts in performing force-spectrum computations, it is necessary to reduce the derived equations into the forms of nomograms or charts so that lengthly computations can be avoided.

All equations listed in Table 1 contain a frequency dependent and a frequency independent term. Therefore, by evaluating the frequency independent terms, and later, combining with the frequency dependent term, the impedance curve can be easily constructed. The approaches, which are based on the separation of the frequency dependency to simplify the impedance prediction, are presented below.

Nomographic Charts — A nomograph, in its simplest and most common form, is a chart on which one can draw a straight line that will intersect three or more scales in values that satisfy an equation or a given set of conditions. The equations summarized in Table 1 were converted into nomographic forms, and are shown in Figures 3 through 8. Figure 3 evaluates the static stiffness of the ring frame. By knowing the values of radius, R, and the flexibility, EI, of the ring, and connecting these two values on the R scale and the EI scale with a straight line, the intersection point in the K scale represents the computational result of the given equation.

Figures 4 and 5 perform similar computations for static stiffness of beams and the frequency independent part of rings, respectively.

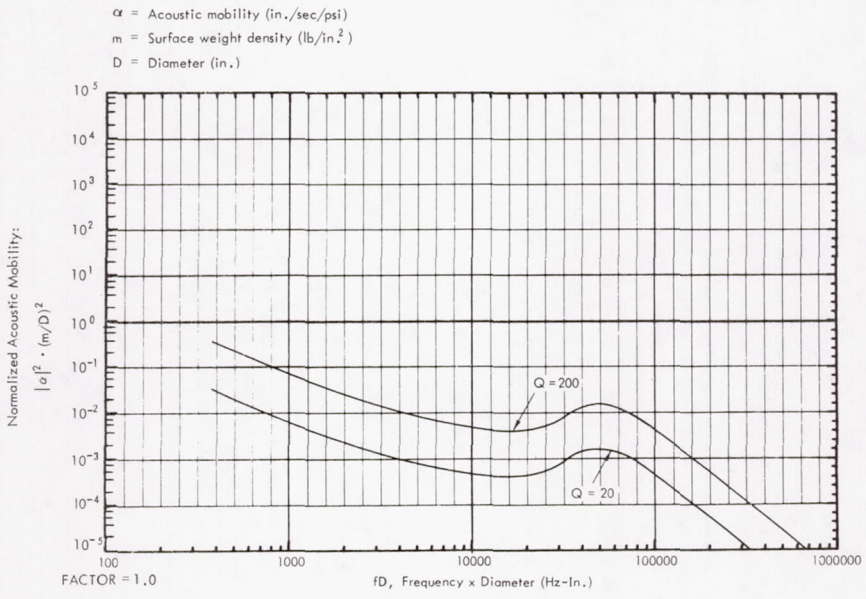

Figure 2. Velocity Acoustic Mobility Levels for Cylindrical Structures (Based on Blocked Pressures)

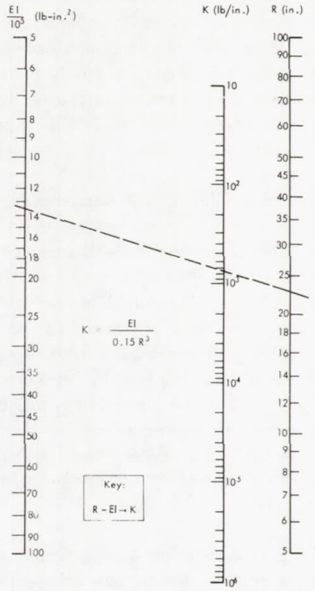

Figure 3. Nomograph for Determining Static Stiffness of Rings

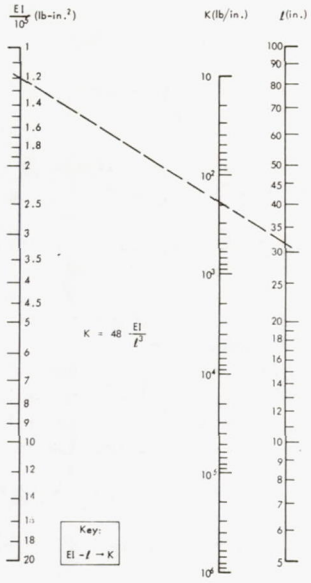

Figure 4. Nomograph for Determining Static Stiffness of Beams

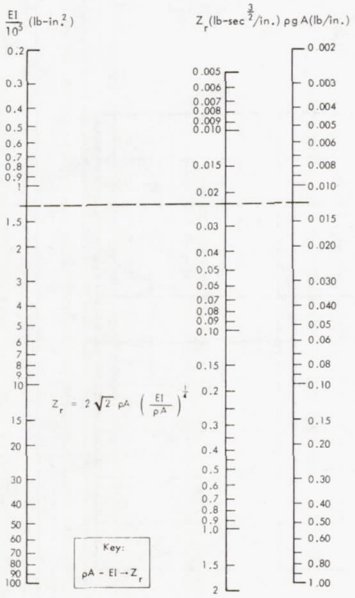

Figure 5. Nomograph for Determining Z_r of Beams and Rings

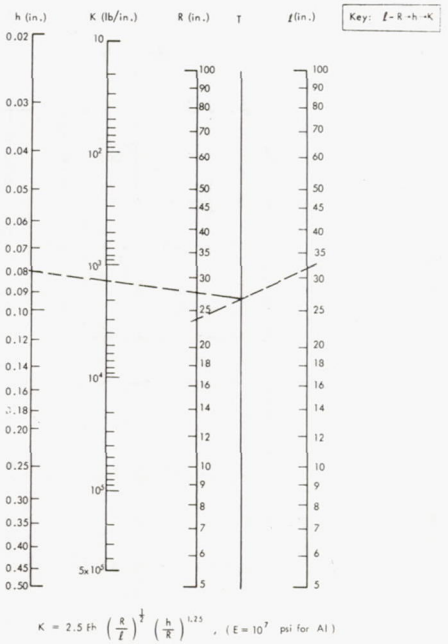

Figure 6. Nomograph for Evaluating Static Stiffness of Unstiffened Cylinders

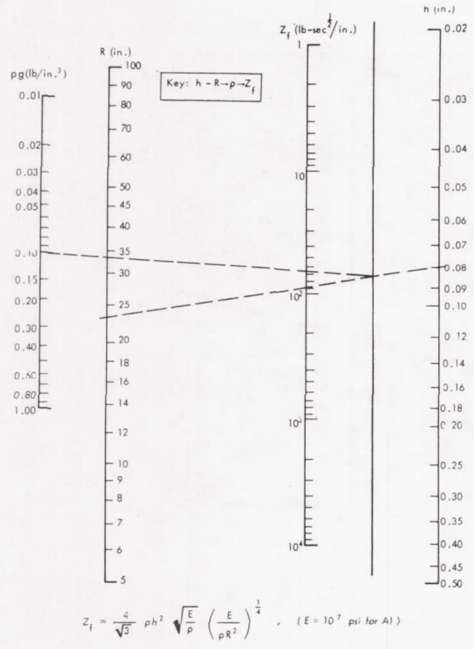

Figure 7. Nomograph for Determining Z_f of Unstiffened Cylinders

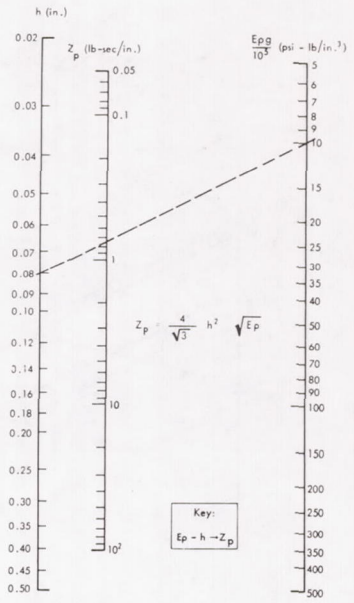

Figure 8. Nomograph for Evaluating Impedance of Infinite Plate

Figures 6, 7 and 8 are four-variable type nomograms for evaluating the frequency independent part of the remaining equations shown in Table 1. For example, in Figure 6, by using one additional axis, T, which lies between the ℓ and R axes and need not be graduated, the four-variable equation was broken into two three-variable equations and are handled as the proceeding way, i.e., connecting the ℓ scale and the R scale with a straight line, then joining the intersection point on the T axis and the h scales with another straight line, the intersection point on the K scale is the resulting value.

Charts for Computing Structural Impedance — The impedance of an ideal damping, spring and mass system may be represented by three intersection lines. By using this approach, the driving-point impedance for beams and rings based on the equations of Table 1 can be represented by two sets of intersection lines varying with the frequency as shown in Figure 9. In this figure, the line representing the proper stiffness value is obtained either from the result of Figures 3 or 4 for rings and beams, respectively, and the line defining the proper Z_r value of the structure is determined from Figure 5. The stiffness lines represent the impedance at low frequencies and the Z_r lines represent the impedance at high frequencies. The intersection of these two lines determines the fundamental resonant frequency of the structural system. In this figure and the following figures, a scale factor is used to obtain correct scale values for the standard diagrams.

The driving-point impedance for unstiffened cylindrical shells is shown in Figure 10, where the Z_r lines are replaced by the Z_f lines. The lines represented the proper stiffness, Z_f, and infinite-plate impedance are obtained from Figures 6, 7 and 8, respectively. At low frequencies, the impedance of cylinders follows a stiffness line and at high frequencies the impedance is equal to the impedance of an infinite plate which has a constant value. Within the intermediate frequency range, the input impedance may be represented by the Z_f line.

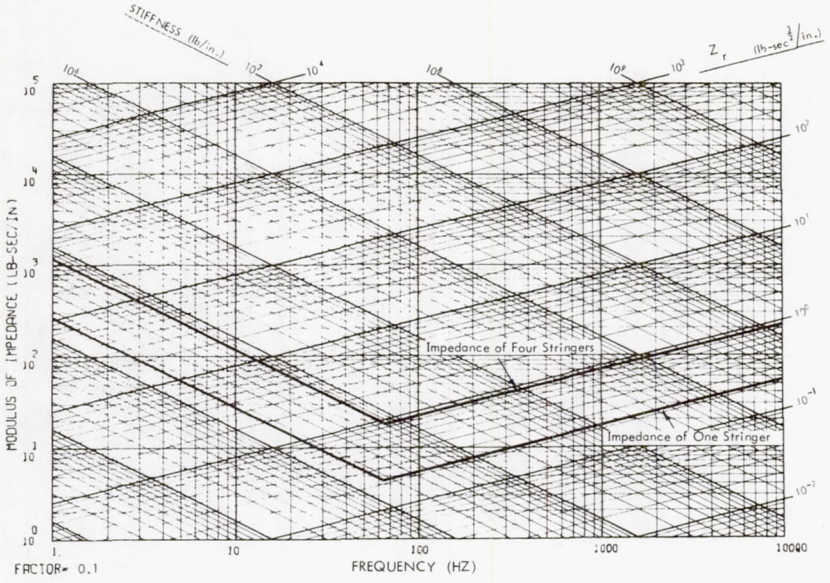

Figure 9. Impedances of Stiffeners

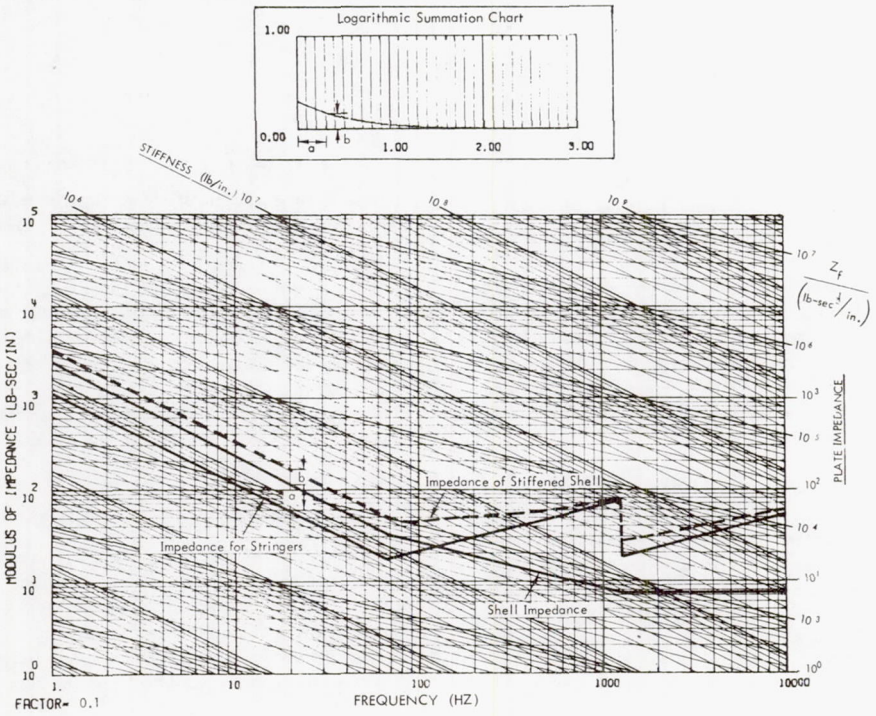

Figure 10. Impedance of Cylindrical Shell

The fundamental frequency and the ring frequency of cylinders are determined by the intersection of these three characteristic lines.

Figure 11 represents the impedance curves for the component package which are defined as an ideal damping, spring and mass system. The graph shown on the upper portion of these two charts will be used to compute the logarithmic sums of two impedance curves. The application of the logarithmic summation chart is explained in example problems.

Charts for Computing Blocked Pressure Spectrum — The conversion of a far-field sound pressure spectrum into a corresponding blocked pressure spectrum is achieved by multiplying the far-field spectrum by the correction coefficient, β, as described in Equation (7). To facilitate graphical computation, Equation (7) is converted to Figure 12, in which the abscissas scale is expressed in terms of fD; where f is the frequency in Hz, and D is the cylinder diameter in inches. To obtain the $\sqrt{\beta}$ - coefficient for a particular cylinder in the frequency scale, it is accomplished by shifting the fD scale in Figure 12 to the left for the amount corresponding to the cylinder diameter, D. For example, if the diameter of a cylinder is 36 inches, the $\sqrt{\beta}$ - coefficient for that cylinder is obtained by shifting the fD scale by a factor of 36 to the left, as shown by the $\sqrt{\beta}$ - curve in Figure 13. The blocked pressure spectrum of the far-field pressure spectrum is then obtained by adding the $\sqrt{\beta}$ values at each frequency point to the far-field pressure spectrum.

Charts for Computing Response Spectrum — The velocity response spectrum is obtained by the product of the blocked pressure spectrum and the velocity acoustic mobility. The normalized acoustic mobility curves as shown in Figure 2 must be converted to $|\alpha|^2$ versus frequency format for use in response computation. The conversion can be accomplished graphically by shifting the abscissas scale to the left corresponding to the diameter of a cylinder, D; and shifting the ordinate scale downward corresponding to the quantity $(m/D)^2$. For example, by applying the above procedures to an aluminum cylinder with D = 36 inches, Q = 20, and $(m/D)^2 - 10^{-6}$ lb/in.^{3}, the velocity mobility for the cylinder curve is obtained as shown in Figure 14. The velocity response spectrum is obtained by summing up logarithmically the velocity acoustic mobility curve and the blocked pressure spectrum curve. The response spectrum is indicated by the dashed-line.

Chart for Computing Force Spectrum — The response spectra and the structural impedance obtained from Figures 14 and 11, respectively, are again plotted on Figure 15 for final computation. The curve representing the sum of these two curves is the resulting force spectrum for the design structural system. Note that all charts developed are in same length scale and the transfer of data curves from one chart to next chart can be easily done by overlay technique.

EXAMPLE PROBLEMS

To aid in understanding the computation procedure, two examples are illustrated. The first example is used to demonstrate the procedures used to predict structural impedances of a stiffened cylinder. The predicted results were then compared with the measured data [5] to evaluate the accuracy of impedance prediction equations. The second example is used to illustrate the procedures in computing a force spectrum based on the structural configurations and the loading criteria used in Reference 2. The measured force response data was used to evaluate the accuracy and conservatism of the predicted force spectrum.

Example of Prediction of Structural Impedance

The specimen used in the prediction consists of a basic cylindrical shell, four longitudinal stringers and two ring frames. The basic cylindrical shell has overall dimensions of 96.0 in. (length) x 48.0 in. (diameter) x 0.08 in. (wall thickness). All structural elements were made of aluminum. The ring frames are built-up channel sections which are attached to the inside surface of the shell wall by means of rivets; and, the stringers are angle sections which are similarly attached to the outside surface of the shell wall. Two heavy end rings consisting of angle sections were welded to the inside surface at the two ends of the shell wall; and, thick circular plywood bulkheads were bolted to the end rings, and are used to provide radial constraint at the ends of the shell wall. Overall dimensions of the specimen are listed in Table 2.

The computations of static stiffness, Z_r and Z_f for the primary structure components have been demonstrated previously as shown in Figures 3 through 8. The impedance computations for the configuration with two ring frames and four stringers are illustrated in Figures 9 and 10. In these two figures, the plotting scale is 10 times the true value as denoted by Factor = 0.1. In the computation, it was assumed that these two rings act like end bulkheads with high structural rigidity so that the effective length of cylinder becomes the length of the middle segment which is equal to 32 inches. In Figure 9, the impedance for one stringer and four stringers are plotted based on the values obtained from Figures 4 and 5. Similarly, the impedance curve representing the unstiffened cylindrical shell is plotted in Figure 10, in which the impedance representing the sum of four stringers is also shown, except that at high frequencies where the structural system decouples dynamically, and the impedance

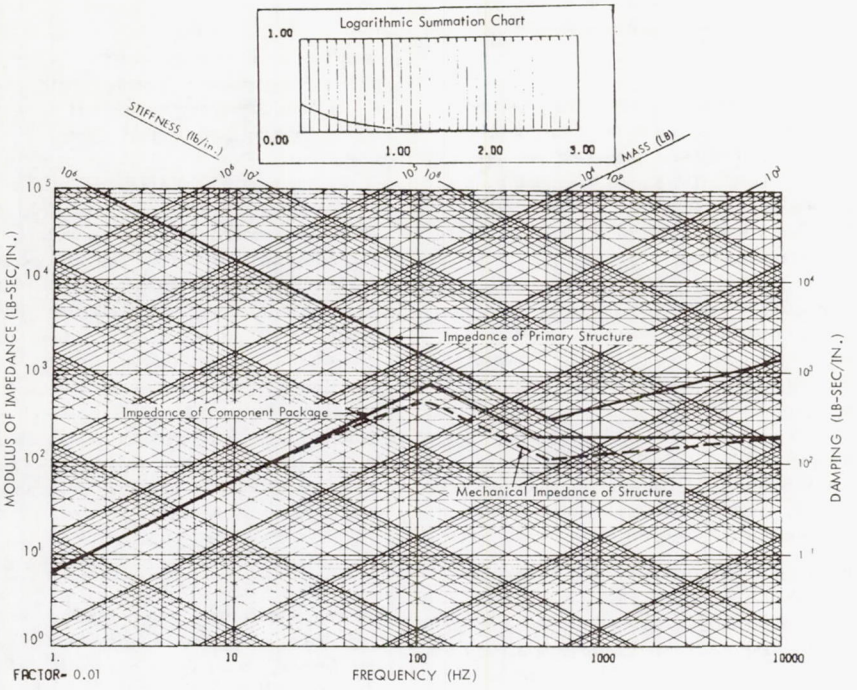

Figure 11. Determination of Structural Impedance

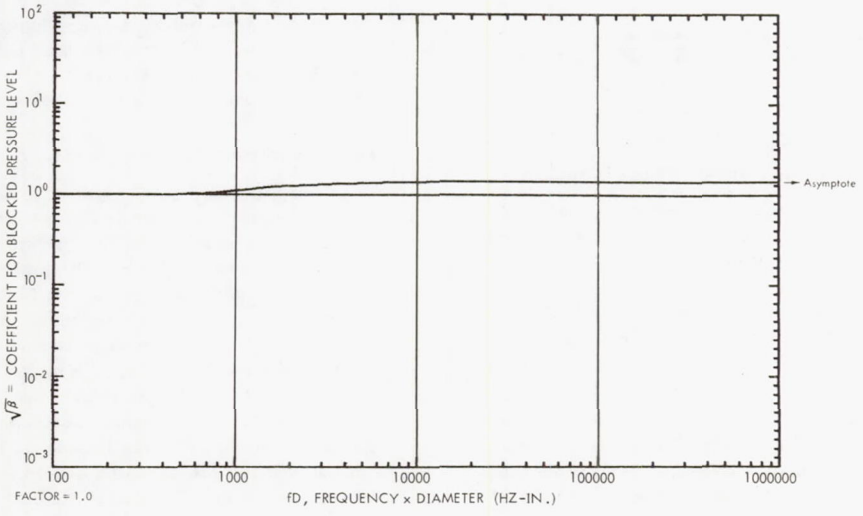

Figure 12. Theoretical $\sqrt{\beta}$ -Curve for Obtaining Blocked Pressure Level of a Cylinder in a Random Sound Field

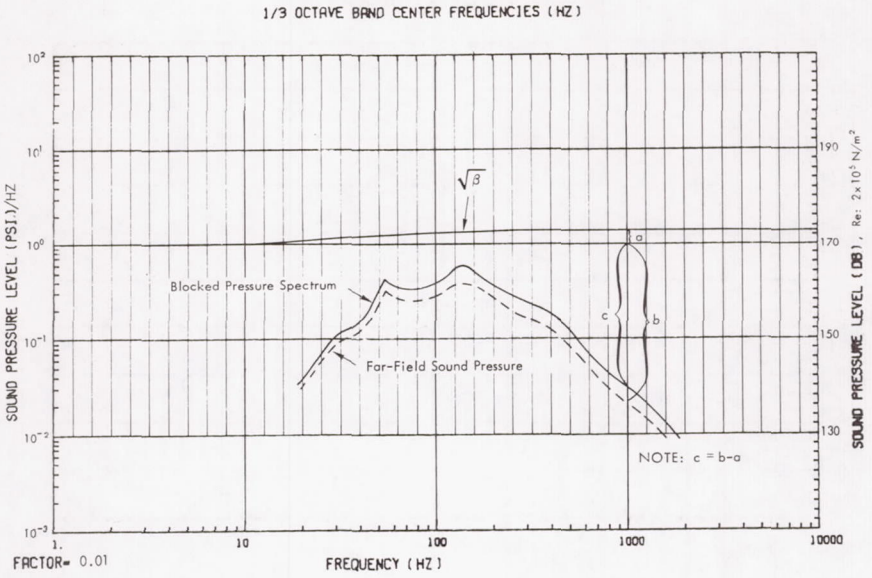

Figure 13. Determination of Blocked Pressure Spectra

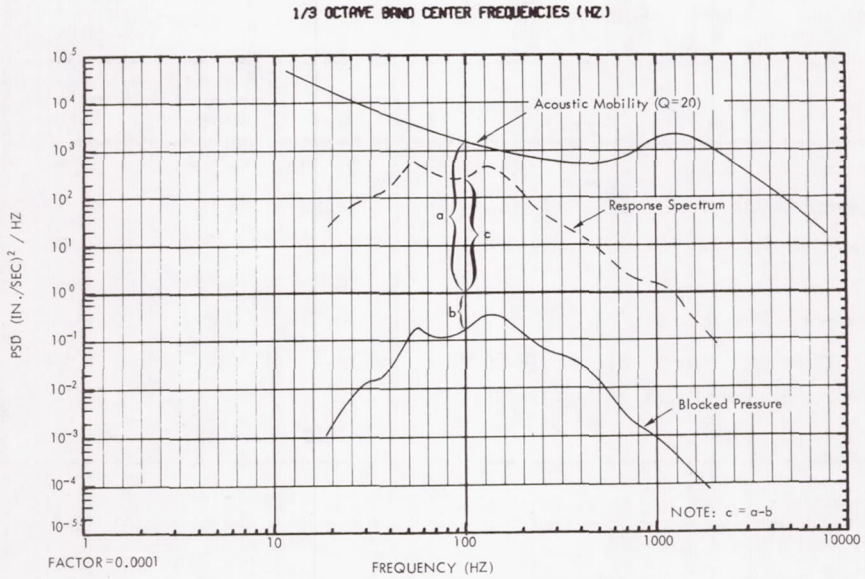

Figure 14. Determination of Structural Response Spectra

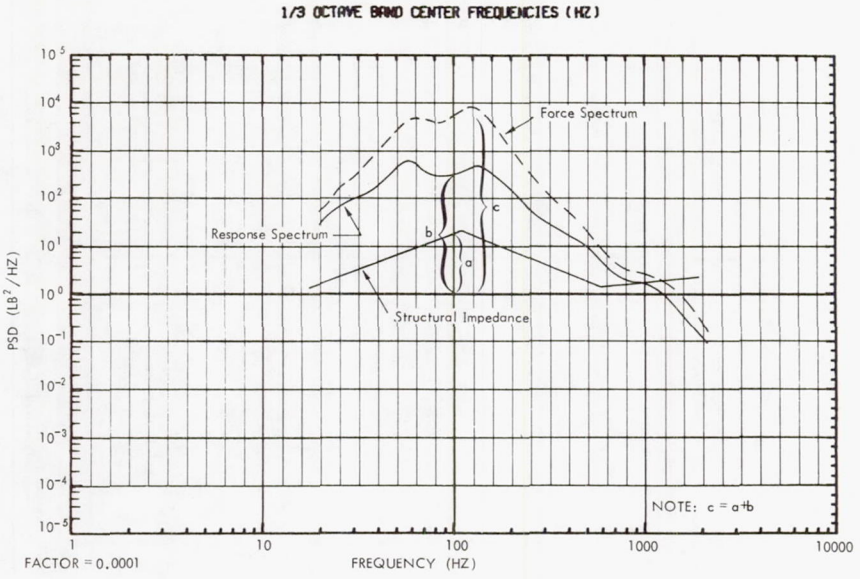

Figure 15. Computation of Force Spectra

TABLE 2. SUMMARY OF DIMENSIONS, STIFFNESS AND MASS PROPERTIES OF CYLINDER AND ITS COMPONENTS

Property	Dimension	Structural Items		
		Ring	Stringer	Shell
Mean Radius, R	(in.)	23.0	---	24.0
Overall Length, ℓ	(in.)	144.5	96.0	96.0
Shell Skin Thickness, h	(in.)	---	---	0.08
Cross-section Area, A	($in.^2$)	0.215	0.123	---
Moment of Inertia, I	($in.^4$)	0.135	0.012	---
Weight per Unit Volume, pg	($lb/in.^3$)	0.1	0.1	0.1
Modulus of Elasticity, E	($lb/in.^2$)	10^7	10^7	10^7
Weight per Stiffener *	(lb)	3.10	1.18	116.0

* Two rings spaced at 32" in the longitudinal direction and four longitudinal stringers spaced at 37.7" in the circumferential direction.

approaches that of one stiffener only. The impedance of the stiffened shell as shown in Figure 10, is equal to the linear summation of these two component impedance curves and it is obtained in the following way:

- At any frequency point, measure the difference of two impedance values and use this length as the abscissas value in the logarithmic summation chart (LSC).
- The ordinate corresponding to the abscissas in the LSC is the resulting value for these two curves in logarithmic summation.
- Add the length of the ordinate to the upper impedance curve, the resulting curve denotes the linear combination of these two impedances.

Figure 16 shows the experimental impedance data obtained from Reference 5 along with the predicted impedance for comparison. Generally speaking, the comparison is considered quite satisfactory both in low frequency and high frequency ranges. Fair agreement is also observed for frequencies just below the ring frequency. Some discrepancies are observed in the intermediate frequency region. Such discrepancies are attributed to the errors incurred in summing the impedances of the stringers. However, it may be concluded that the equation and guidelines presented are adequate for determining the structural impedances for design purposes.

Example for Prediction of Force Spectra

The structure used in the second example was a stiffened aluminum cylinder whose dimensions were 36.0 in. (diameter) x 36.0 in. (length) x 0.02 in. (thick). The cylinder consisted of five aluminum rings spaced at 6 inches in the longitudinal direction, and 24 longitudinal stringers spaced at 4.7 inches in the circumferential direction. All stiffeners were mounted to the cylinder wall by rivets. The dimensions of the curved panels formed by the stiffeners were 6 inches and 4.75 inches. Two steel rings of angle sections were rivetted at both ends and two circular sandwich plates were bolted to the end rings.

The simulated component package consisted of a 1/2 in. aluminum plate with lateral dimensions of 8.0 in. x 8.0 in. The plate was supported by four sets of leaf springs at its corners. The bottom of each spring was fitted with a load washer assembly. The total weight of the component package was 3.81 pounds; the resonant frequency of the package was measured at 110 Hz.

In order to estimate the force spectra, the analytic procedures used to predict the impedance of the stiffened cylinder are essentially the same as that described in the preceding example. Hence, no analytical prediction was made and the impedance was obtained from the experimental testing. The impedance of the component package is estimated and is shown in Figure 11. The measured impedance for the stiffened cylinder is also presented in the same figure, which is approximated by two inclined straight lines as shown. In this figure, the plotting scale is 100 times the true value as denoted by Factor = 0.01. These two impedance curves are then combined according to the logarithmic summation technique as described for the impedance of the stiffened shell except that the resultant curve is obtained by subtracting the length of the ordinate coordinate from the lower impedance curve, i.e., by summing the two individual mobility curves. The summed curve given is the impedance term in the computation of the force-spectra equation.

The measured sound pressure and the blocked pressure spectra for this example have been obtained according to the procedure as described previously and the results are shown in Figure 13. The response spectrum is then obtained by summing the acoustic mobility curve and the blocked pressure curve as shown in Figure 14. The resulting curve as shown in Figure 15 is the computed force spectrum. In Figures 14 and 15, the plotting scal scale is 10,000 times the correct value as denoted by Factor = 0.0001. The measured force response spectrum obtained from Reference 2 is shown in Figure 17 along with the computed force spectrum. The predicted force spectrum was slightly high, but was judged to be acceptable, since the computed results provide the more conservative estimate for design evaluation.

CONCLUSIONS

A simplified procedure has been developed to predict the interaction force between a component and its support structure (space vehicle) which is subjected to broadband random acoustic excitations. This method was derived from a one-dimensional impedance model and the computation was performed by ways of nomograms and design charts. The conclusions resulting from this study are:

- The force-spectrum equation provides satisfactory results on the predicted force environments of components mounted on space vehicles. This equation is valid for the prediction of forces in the radial direction of the support structure. However, the same concept can be expanded to include the coupling effects induced from the longitudinal and tangential directions so that the complete description of forces in all three directions is feasible.
- The simplified computation method as presented has been shown to be accurate and conservative within current acceptable tolerance limits. The computation process requires minimum manual effort and no computer assistance is required.

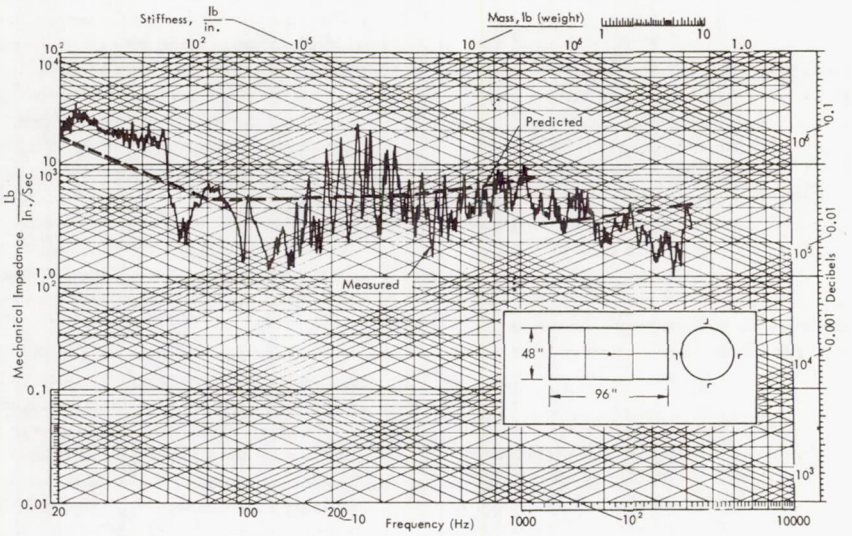

Figure 16. Measured Input Impedance: Shell with Two Rings and Four Stringers (Reference 5)

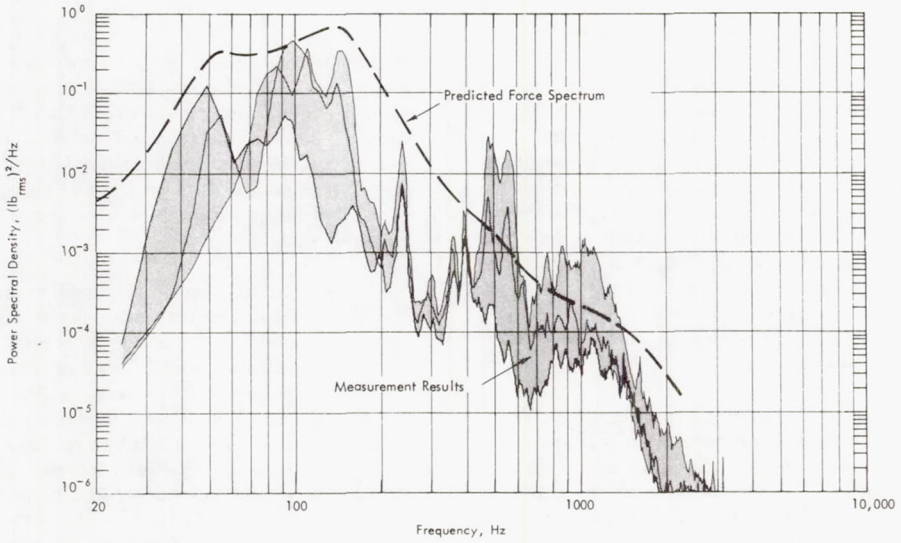

Figure 17. Measured Force Spectrum (Reference 2)

ACKNOWLEDGMENTS

This work was sponsored by National Aeronautics and Space Administration, Marshall Space Flight Center, Huntsville, Alabama, under Contract No. NAS8-25811.

REFERENCES

1. Barrett, R.E., "Techniques for Predicting Localized Vibratory Environments of Rocket Vehicles," NASA TN-D-1836, October 1963.

2. Kao, G.C., "Prediction of Force Spectra by Mechanical Impedance and Acoustic Mobility Measurement Techniques," Wyle Laboratories Research Staff Report WR 71-16, October 1971.

3. Chang, K.Y., Cockburn, J.C. and Kao, G.C., "Prediction of Vibro-Acoustic Loading Criteria for Space Vehicle Components," Wyle Laboratories Research Staff Report WR 73-9, September 1973.

4. Waterhouse, R.V., "Diffraction Effects in a Random Sound Field," JASA, Vol. 35, pp. 1610-1620, October 1963.

5. Conticelli, V.M., Kao, G.C. and White, R.W., "Experimental Evaluation of Input Impedances of Stiffened Cylindrical Shells," Wyle Laboratories Research Staff Report WR 70-12, August 1970.